

# Single-Point-Attachment Wind Damper for Launch Vehicle On-Pad Motion

Glenn A. Hrinda<sup>1</sup>

NASA Langley Research Center, Hampton, Virginia, 23681

A single-point-attachment wind-damper device is proposed to reduce on-pad motion of a cylindrical launch vehicle. The device is uniquely designed to attach at only one location along the vehicle and capable of damping out wind gusts from any lateral direction. The only source of damping is from two viscous dampers in the device. The effectiveness of the damper design in reducing vehicle displacements is determined from transient analysis results using an Ares I-X launch vehicle. Combinations of different spring stiffnesses and damping are used to show how the vehicle's displacement response is significantly reduced during a wind gust.

## Nomenclature

$c$	=	damping coefficient (lb-s/in)
$f$	=	frequency
$FEM$	=	finite element model
$FSS$	=	Fixed Service Structure
$ISS$	=	International Space Station
$K$	=	spring coefficient (lb/in)
$LAS$	=	Launch Abort System
$MLP$	=	Mobile Launch Platform
$RSS$	=	Rotated Service Structure
$SRB$	=	Solid Rocket Booster
$\xi$	=	viscous damping factor

## I. Introduction

Long cylindrical space launch vehicles, such as the Ares I<sup>1</sup>, may experience damaging dynamic loads from ground winds before launch. Wind gusts can oscillate near a natural resonance of the launch vehicle creating excessive motion that exceeds structural design limits. This may include high stress levels in launch vehicle structures or design clearances between the launch tower and the vehicle to be compromised. Previous launch vehicle designers considered the possibility of high ground winds preceding a launch.<sup>2</sup> They produced wind damper designs that could be placed between a launch tower and vehicle to minimize wind induced motions. An example is the wind damper used on the Apollo Saturn V shown in Fig. 1.<sup>3,4</sup>

---

<sup>1</sup> Structural Engineer, Vehicle Analysis Branch, MS 451.

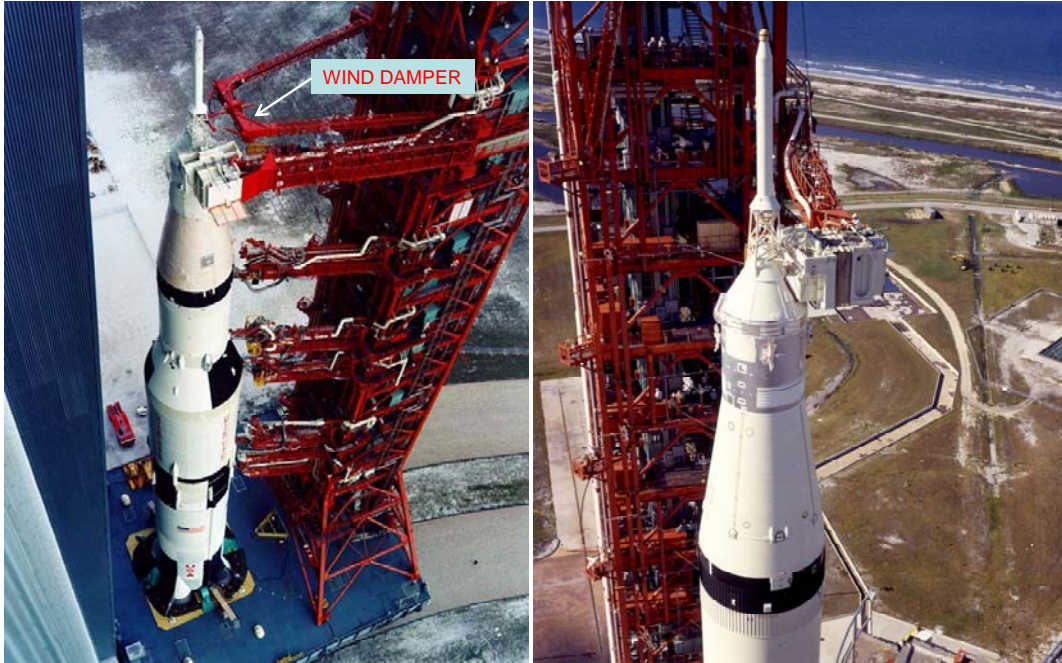


**Figure 1. Apollo Saturn V wind damper. The left photograph shows the wind damper extended and attached to the launch abort tower of the Saturn V. The wind damper has been retracted just prior to launch in the right photograph.**

The launch of Skylab in May 1973 also showed how designers addressed the ground wind problem. The photograph in Fig. 2 shows a wind damper attached to the tip of the Skylab Saturn V that was similar to the Apollo design.

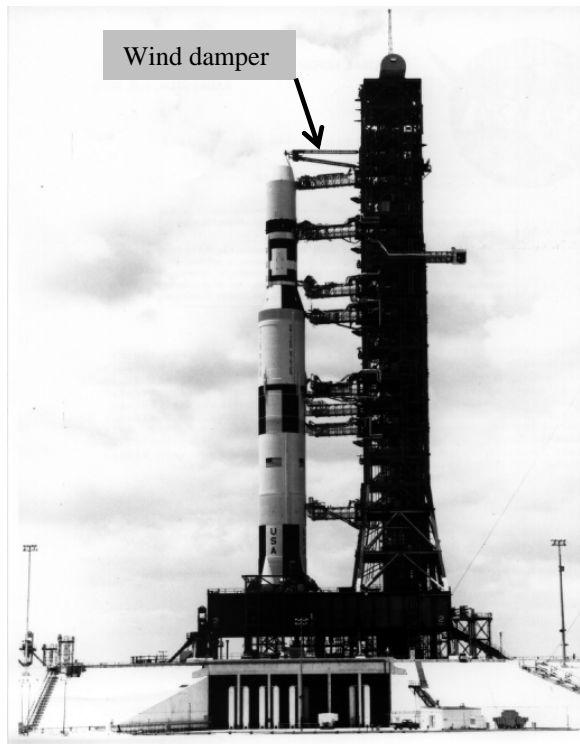


**Figure 2. Skylab Saturn V wind damper.**

The Atlas V is a more recent space launch vehicle that also has a wind damper. Figure 3 shows the vehicle and location of the wind damper. The damper device was provided by Taylor Devices Inc.<sup>5</sup> and differs from the Apollo designs. The Atlas V device attaches at a single point and provides viscous damping.

The next generation space launch vehicle currently under design by NASA is the Ares I. The vehicle will launch astronauts in the Orion crew module to the *ISS* (International Space Station) and also on lunar missions. The development of the new launch vehicle includes a flight test called the Ares I-X. Data obtained from this test will help prove the components of the Ares I crew launch vehicle. The Ares I-X is the first in a series of flight tests necessary to qualify the Ares I design.<sup>6</sup> During the development of this first flight test, wind loading became increasingly important to understand. This paper documents an investigation that was performed to find methods for analyzing ground wind effects and potential attenuation designs. The load profile was determined from prior KSC analysis models and given by KSC to use in this analysis.<sup>7</sup> Figure 4 shows the Ares I-X prior to launch. The vehicle utilizes Space Shuttle launch hardware with additional modifications for a wind damper. This analysis investigated two possible methods for attaching a wind damper to the launch tower hardware. The first method is given in Fig. 5 and shows a dedicated umbilical extending from the Shuttle launch tower. This design required new support structure for attaching a damper device. The concept was rejected by the project office because of concerns that the existing launch tower structure would require extensive modification.



**Figure 3. Atlas V wind damper.**



**Figure 4. Ares I-X.**

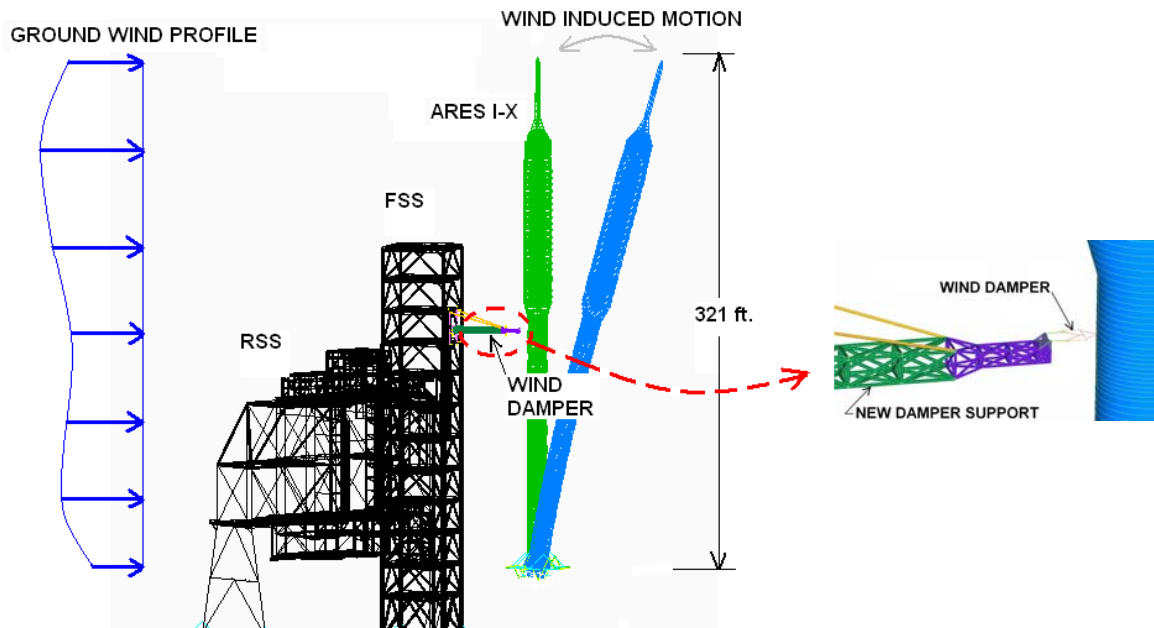


**Figure 5. Ares I-X and existing Space Shuttle launch structure FEM with the addition of a new wind damper (concept 1).**

A second method was conceived that did not attach to the existing launch tower, but rather a new tower. Figure 6 shows the new tower concept next to Ares I-X and the existing Space Shuttle launch hardware. The tower was placed over the opposite Space Shuttle *SRB* exhaust hole on the *MLP*. This was the design that was analyzed and is explained in the following sections.

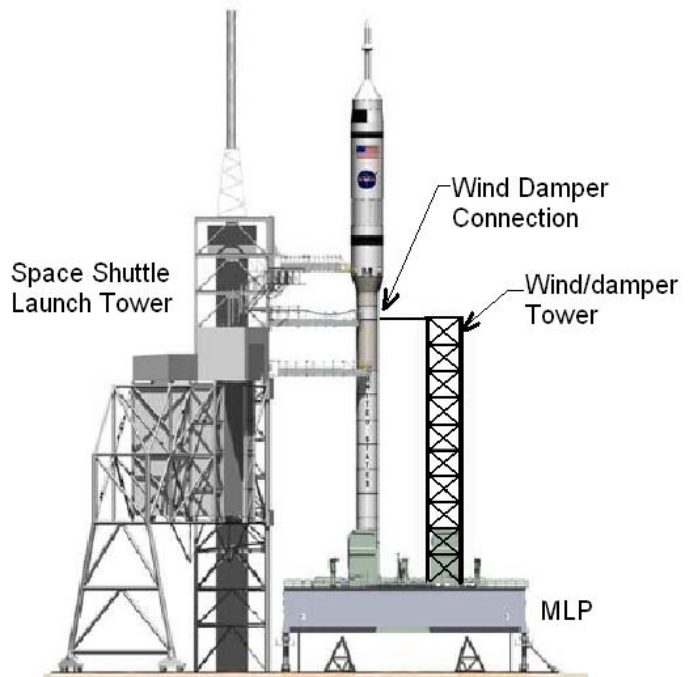


**Figure 6. Ares I-X on MLP with existing Shuttle tower and new wind/damper tower using concept 2.**



## II. Analysis

The start of the analysis required finding the main bending modes of the Ares I-X with spring constants at the four hold-down bolt locations shown in Fig. 7. The locations of the bolts were identical to the existing Space Shuttle hold-down bolts.<sup>8</sup> Their location produced a strong and weak axis bending of the vehicle under ground wind loads. Strong axis bending was produced when the wind load was near  $0^\circ$  as shown in Fig. 8. This caused the launch vehicle to bend about the strong axis at the bottom of the SRB skirt. When the wind load was applied at  $90^\circ$

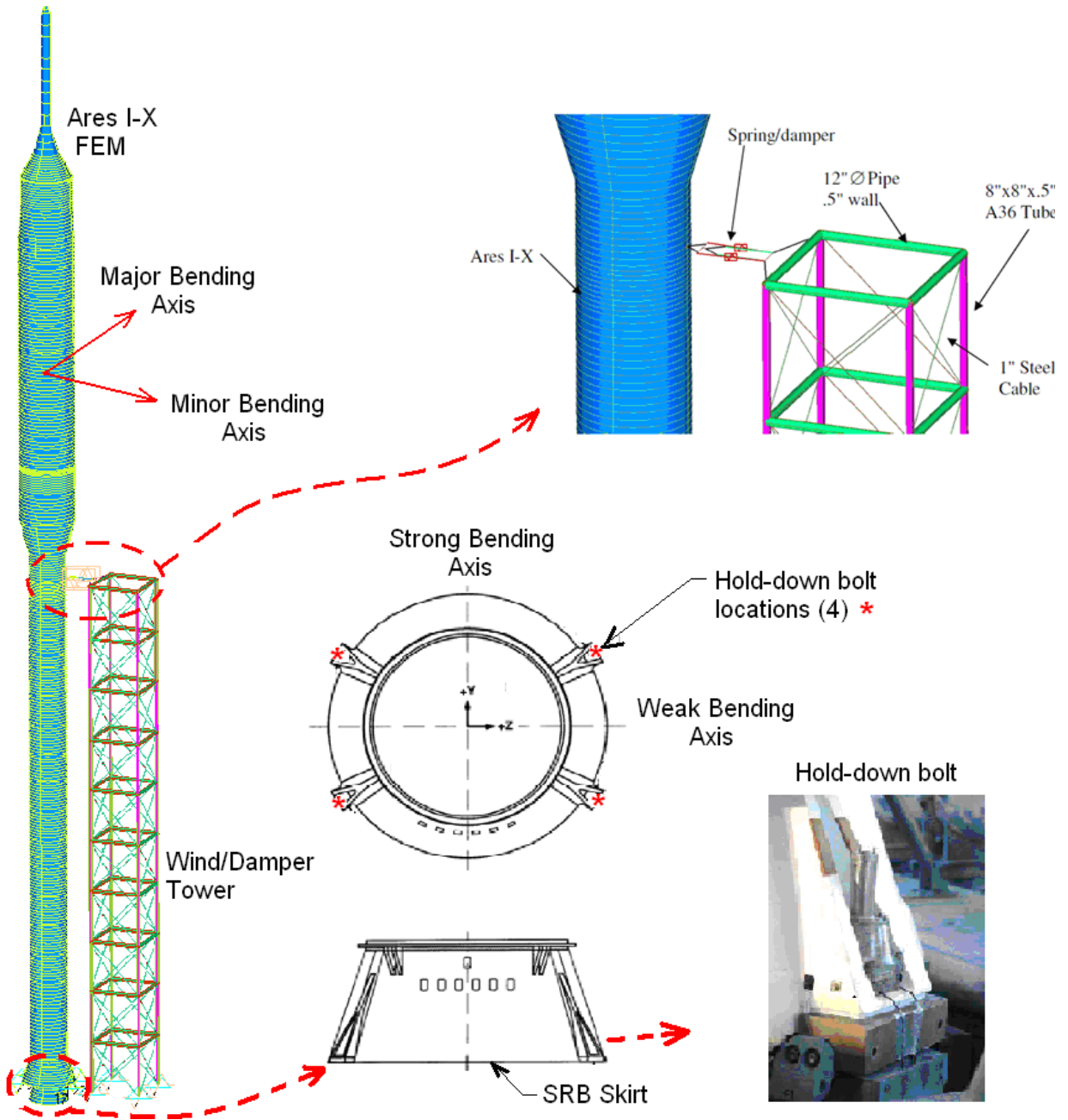
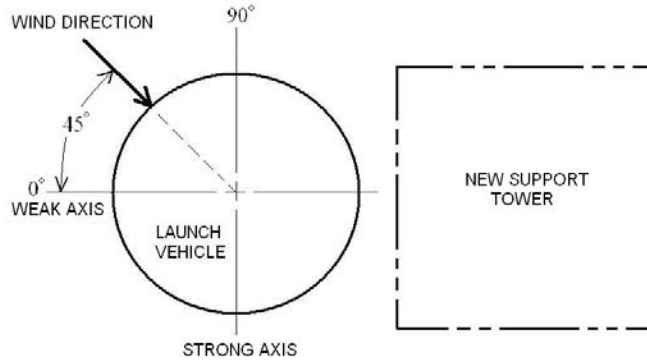
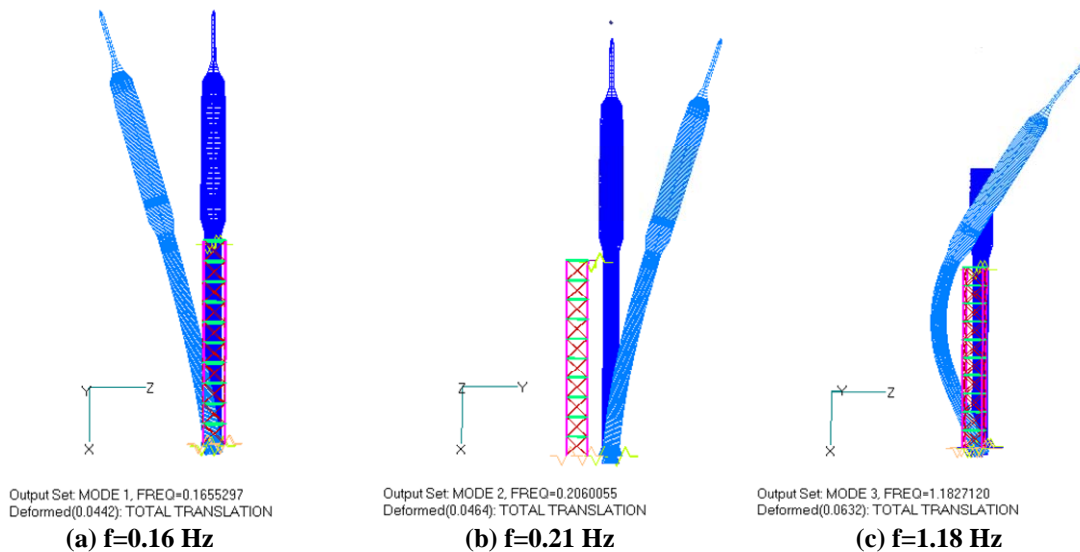


Figure 7. Ares I-X and tower FEM showing hold-down bolts.

as shown in Fig. 8, the launch vehicle would bend about the weak axis at the base of the *SRB* skirt. This caused the launch vehicle to bend along a path that was parallel to the tower. The main cause for asymmetric bending was the different off-centerline distances of the hold-down bolts. Figure 9 shows the first three bending modes of the launch vehicle with the hold-down bolts modeled as springs. The first mode bending frequency of 0.16 Hz was about the weak axis shown in Figs. 7 and 8. The second mode had a bending frequency of 0.21 Hz and was about the strong bending axis. The third mode was 1.18 Hz and had a second bending shape about the weak axis. These modes are shown in Fig 9.



**Figure 8. Wind gust directions.**



**Figure 9. Bending modes of free-standing vehicle.**

The next step was a direct transient analysis performed to characterize a peak on-pad ground wind gust over a 10-day period using a Nastran<sup>9</sup> finite-element model (*FEM*). The load was a single sine pulse of amplitude that equaled a 10-day ground wind gust profile and at a frequency that equaled the first bending mode of the freestanding Ares I-X.<sup>7</sup> The ground wind gust used in this analysis was the maximum wind gust that could occur while the Ares I-X was on the pad for no longer than 10 days with a 1 percent chance that the peak gust would be exceeded. Later in the development program this requirement was changed to a 30-day pad stay. The load profile was determined from prior KSC analysis models and provided for use in this analysis.

### III. Launch Vehicle and Wind Damper FEM

The Ares I-X *FEM* was a representative math model of the Ares I-X flight-test vehicle. The model consisted mostly of beam elements and lumped masses to closely approximate the Ares I-X stack.<sup>8</sup> The four hold-down springs at the base of the stack model were modeled from Space Shuttle data.

The spring/damper device design was modeled with Nastran<sup>9</sup> beam, springs, and damper elements in conjunction with appropriately restrained rigid elements. Figure 10 shows the spring/damper device with Fig. 11 indicating the degrees of freedom that were permitted to allow axial attenuation in the spring and damper elements, as well as in-plane rotation of the attachment arms.<sup>5</sup> This arrangement allowed attenuation of launch vehicle motion from wind gusts in any direction. The damper attachment to the vehicle and the new tower are shown in Fig. 7. The attachment was located at a stiffened ring frame in the vehicle and could not be relocated. Also shown are the sizes of the members that were used in the new tower and the rigid elements that were used to connect the damper to the tower. These sizes provided sufficient stiffness to prevent excessive bending and torsion displacement at the top of the tower.

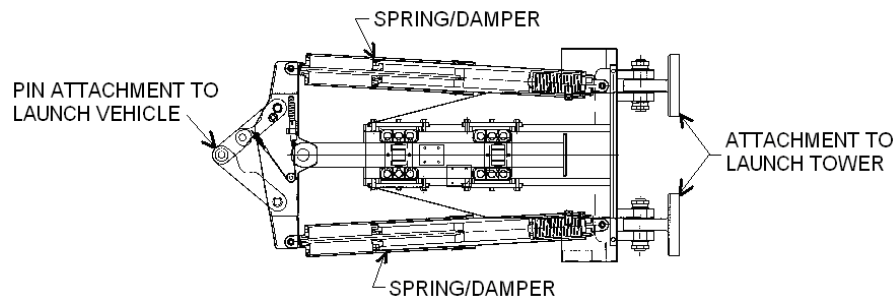


Figure 10. Spring/Damper device.

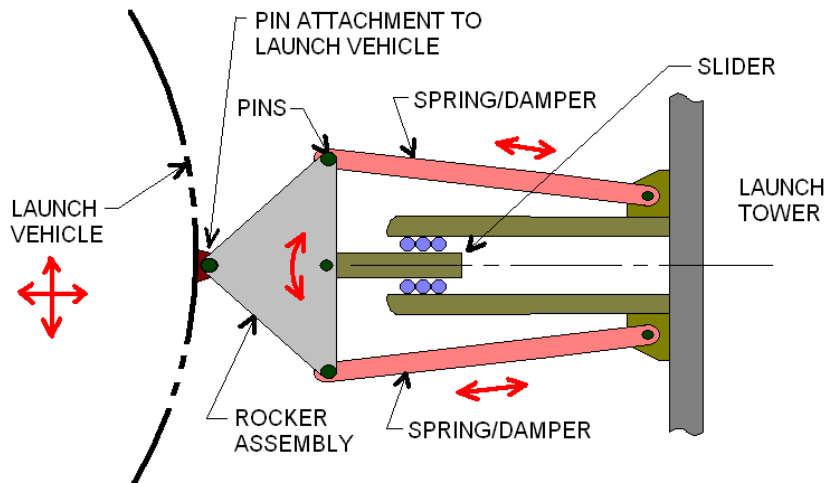


Figure 11. Wind spring/damper device attached at single-point.

#### IV. Wind Gust Modeling

Ground wind loads were applied to the vehicle from three directions:  $0^\circ$ ,  $45^\circ$  and  $90^\circ$ . Figure 8 shows a plan view of the launch vehicle and the three load directions. Each load was applied separately to produce bending of the launch vehicle on the pad. It was found that the ground wind load in the  $90^\circ$  direction produced the largest displacements about the weak bending axis shown in Figs. 7 and 8. This was also the first free-standing bending mode at 0.16 Hz as shown in Fig 9. The applied gust load was tuned to this first bending frequency and used in the transient analysis. Figure 12 shows a 0.16 Hz sine pulse that was used with the gust loading. The analysis used a time step of 0.1 s and was allowed to run for 20 s and 60 s.

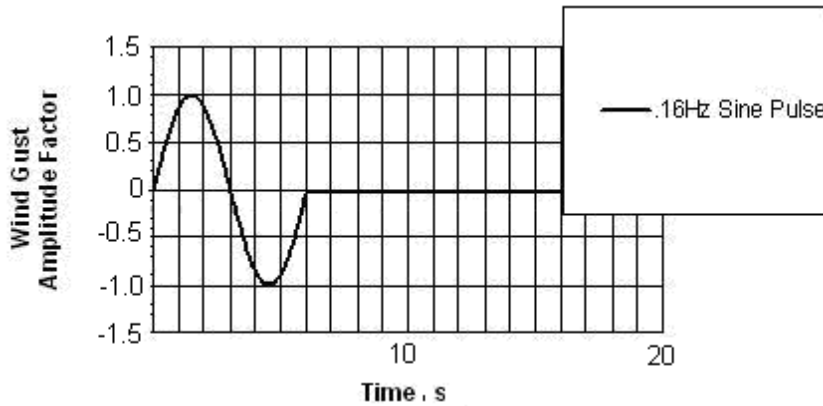


Figure 12. Wind gust load factor.

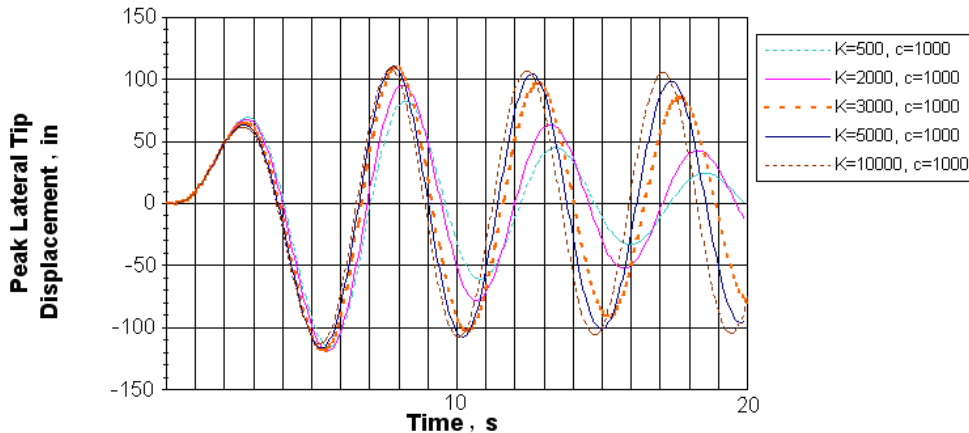


Figure 13. Tip displacements for various spring coefficients in the spring/damper device.



## V. Results

The tip displacement of the vehicle's Launch Abort System (LAS) was tracked to determine the effectiveness of the spring/damper. A series of trade studies produced tip displacements for varying spring coefficients and damping constants for the spring/damper, in addition to a wind/damper tower design. Figure 13 shows multiple plots of the tip displacement time histories. The spring/stiffness values  $K$  are measured in lb/in while the damping coefficient  $c$  is measured in lb-s/in. The reduced displacement amplitudes can be seen, as can the shift in the frequency with variations in the spring/damper stiffness.

The time history of the load that connects the spring/damper to the side of the Ares I-X vehicle is plotted in Fig. 15. This load was transmitted in shear through a pin or bolt at the outer perimeter of the vehicle as shown in Fig. 11. The direction of the load was through the center of the attachment pin and opposite to the wind direction. As one would expect, this load increases when higher spring coefficients are used. The plots closely follow the displacement curves at the tip.

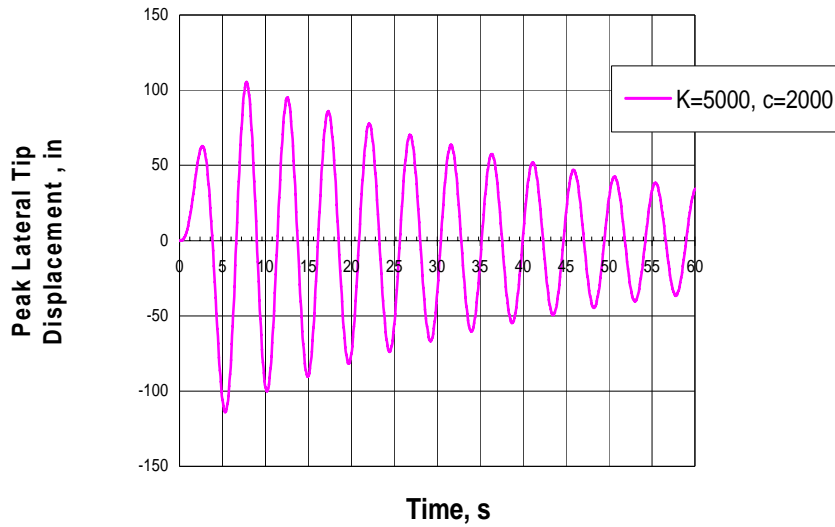


Figure 14. Time history of tip displacement with  $K = 5000$  lb/in &  $c = 2000$  lb-s/in.

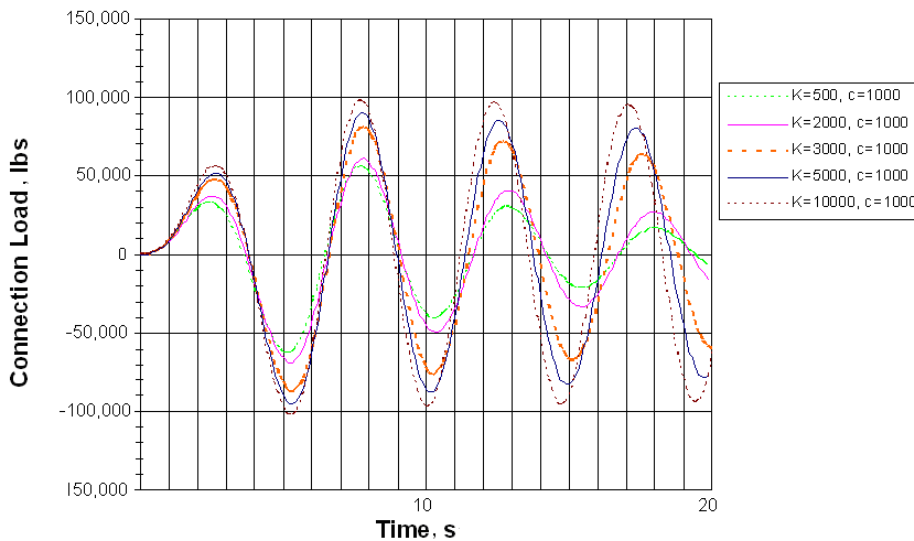


Figure 15. Loads at spring/damper connection to Ares I-X at varying spring coefficients.

The analysis was also performed for several spring coefficients and damping constants with time histories to 60 s. This was done to capture the decay rate of the peak tip displacement and calculate the system damping. The overall damping factor  $\xi$  is determined by the logarithmic decrement technique which assumes viscous damping.<sup>10</sup> Figure 14 shows a 60 s time history for peak tip displacement with a spring/damper that uses  $K = 5000$  lb/in and  $c = 2000$  lb-s/in. A semi-log plot of the peak displacement at each cycle is shown in Fig. 16. The straight-line plot is a good indicator that the system is viscously damped.

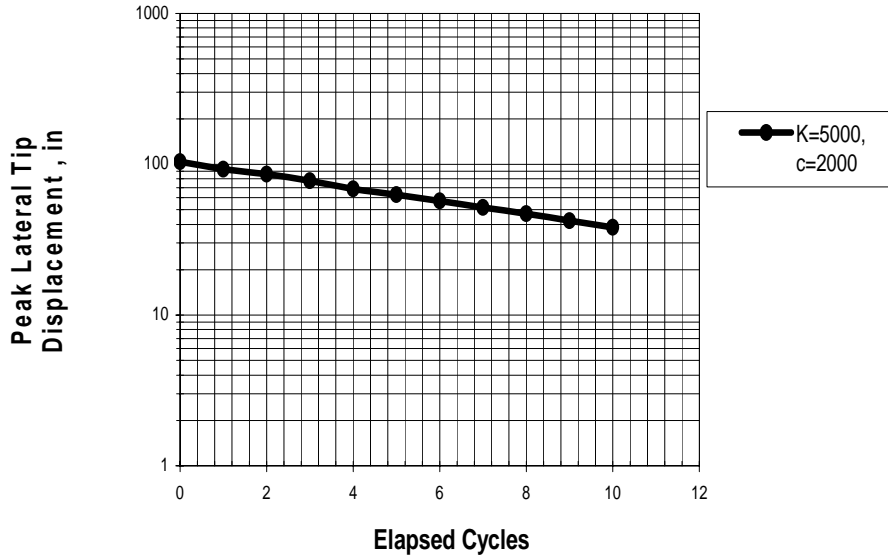


Figure 16. Log decrement for damping.

The viscous damping factor of the system may now be found as

$$\ln\left(\frac{104}{38.3}\right) = 2\xi\pi(10) \quad (1)$$

$$\xi = .016 = 1.6\% \quad (2)$$

## VI. Wind Damper Performance

A summary of the main dynamic parameters that were produced by using the spring/damper design with the new support tower is given in Table 1. The tip displacements and the damping percentages are based on the free response of the vehicle during a 6 s full sine gust and a half sine gust with both tuned to the 0.16 Hz first natural freestanding mode. The system dampings for both types of sine pulses are given and are shown to be nearly equal. This was done to demonstrate that the models behaved as expected and that the logarithmic decrement technique was accurate.

Table 1. Summary of dynamic constants.

$K \left(\frac{lb}{in}\right)$	$c \left(\frac{lb-s}{in}\right)$	$\xi$ (%FEM damping, full sine)	$\xi$ (%FEM damping, half sine)	$\Delta_{Tip}$ (in)		$f_1$ (Hz)
				Full sine pulse	Half sine pulse	
0	0	0.0	0.0	183.70	92.00	0.1655
500	1000	8.0	7.9	82.8	69.4	0.1819
1000	1000	6.4	6.4	95.0	68.0	0.1905
2000	1000	3.3	3.4	106.0	66.2	0.1995
3000	1000	1.97	2.0	108.6	65.0	0.2042
5000	2000	1.6	1.7	104.0	62.9	0.2089

## VII. Discussion

The spring/damper design that is considered in this effort can be used to lower the maximum displacements that result from a 10-day peak on-pad wind gust. The spring/damper device can lower the vehicle tip displacements from 183.7 in. (zero-to-peak) to 82.5 in. (zero-to-peak) for the conservative full sine gust pulse. The spring/damper can also lower the maximum vehicle tip displacements for the half sine pulse from 92.0 in. (zero-to-peak) to 62.9 in. (zero-to-peak). As the spring/damper stiffness increases, a trade-off is noted. Increasing spring coefficients causes the first bending mode to increase but also increases the load at the pin attachment to the launch vehicle in figure 11. The results demonstrate that flexibility exists in the design. A spring rate and damping constant can be selected that can attenuate peak displacements and increase the first bending mode frequency to allow a reasonable design load at the spring/damper connection to the vehicle. The analysis also shows that the system is viscously damped and that the amount of system damping can be controlled to obtain rates of up to 8 percent. One possible design is a wind spring/damper device with a spring rate of 2000 lb/in and a linear damping constant of 1000 lb-s/in. This produces a peak lateral displacement of 106.0 in. at the tip of the LAS, at a first bending mode of almost 0.2 Hz with a systems damping of 3.3 percent.

## VIII. Conclusions

Long cylindrical launch vehicles that are exposed to ground winds may be protected from excessive motion by a single-point spring/damper design. This concept was demonstrated by using a spring/damper device to attenuate the ground wind induced response of an Ares I-X launch vehicle. The device reduced the launch vehicle's on-pad oscillations from varying wind directions with only one attachment point to the vehicle. This feature may have particular interest to designers of future launch vehicles where only a limited number of attachment points are permitted.

## References

- <sup>1</sup>Davis, S. R., "Ares I-X Flight Test-The Future Begins Here," AIAA Paper 2008-7806, September 2008.
- <sup>2</sup>Jones, G. W., Farmer, M. G., "Wind-Tunnel Studies of Ground-Wind Loads on Saturn Launch Vehicles," *AIAA Journal of Spacecraft*, Vol. 4, No. 2, 1967, pp. 219, 223.
- <sup>3</sup>Mackey, A. C., Schwartz, R. D., "Apollo Experience Report-The Development of Design-Loads Criteria, Methods, and Operational and Midboost Conditions Procedures for Prelaunch, Lift-Off, and Midboost Conditions," NASA TN D-7373, 1973.
- <sup>4</sup>NASA Marshall Spaceflight Center, "Saturn V Flight Manual, SA 507", MSFC-MAN-507, 1969.
- <sup>5</sup>Taylor Devices, Inc., "Shock Force, The Marketing Newsletter of Taylor Devices, Inc., Special Edition-NASA Mission", URL: <http://www.taylordevices.com> [cited 20 January 2006].
- <sup>6</sup>NASA Langley Research Center, NASA Facts "Constellation Program: Ares I-X Flight Test Vehicle," FS-2008-04-142-LaRC.
- <sup>7</sup>NASA Marshall Space Flight Center, "Ares I-X Flight Test Vehicle Structures Databook", Document number AII-SYS-SDB, 2006.
- <sup>8</sup>NASA Marshall Space Flight Center, "Ares I Integrated Vehicle Design Definition Document", CxP 72070, 2006.
- <sup>9</sup>NEiNastran User's Manual, Ver. 9.1, Noran Engineering, 2009.
- <sup>10</sup>James, M. L., Smith, G. M., Wolford, J. C., and Whaley, P. W., *Vibration of Mechanical and Structural Systems*, 1<sup>st</sup> ed., Harper & Row, New York, 1989, Chap. 2.